Phonon amplification using evaporation and adsorption of helium

T. More, J. S. Adams, S. R. Bandler,* S. M. Brouër,† R. E. Lanou, H. J. Maris, and G. M. Seidel
Department of Physics, Brown University, Providence, Rhode Island 02912
(Received 28 November 1995; revised manuscript received 26 March 1996)

We report the results of experiments designed to investigate the feasibility of amplifying a phonon signal using the evaporation of helium from a superfluid film and its subsequent readsorption onto a helium-free surface. We envision a multistage amplifier in which helium is evaporated from a wafer with a helium film only on one side and then adsorbed onto the film-free surface of a similar wafer. The phonons created by the adsorption reach the film on the opposite side of the wafer and potentially desorb more helium than was evaporated by the first wafer. The amplification would come from the high ratio of the binding energy of a helium atom to a film-free surface relative to the binding energy to the liquid. A number of experiments are reported that investigate the efficiencies of the individual steps of the process. The gain per stage is found to be about 3 for high-energy densities in which multiphonon processes are possible. At low-energy densities, the energy deposited into a film-free wafer is found to be less than the original input energy, with the ratio of output to input energy 0.2. Since in applications requiring amplification the phonon density produced by the adsorption of helium on a wafer will be low, the configuration we have studied—phonons produced in silicon coated with a saturated ^{4}He film—will not result in amplification. However, other configurations might improve the efficiency enough to make an amplifier possible. [S0163-1829(96)02626-4]

I. INTRODUCTION

Large cryogenic solid-state particle detectors are being developed to determine whether weakly interacting massive particles are a component of the dark matter in our universe.[1] These particles are expected to have a mass between 1 and 100 GeV, a weak interaction cross section, and an average velocity relative to the earth of approximately 230 km/s with some seasonal variation due to the earth's motion around the sun.[2] In a typical detector design, the weakly interacting massive particle interacts in a solid target, causing a nucleus to recoil. The cross section of the interaction of a weakly interacting massive particle with a nucleus in a detector depends on the properties of both the incoming particle and the target material. A reasonable rate (a few events per day) requires a target mass of at least several kilograms. The maximum recoil expected is generally 1 keV or less and appears primarily as phonons in the target. If these phonons were to thermalize in a 1 kg silicon detector at a temperature of 100 mK, the temperature rise would be only about 0.6 nK. In fact, the phonons do not thermalize before reaching the target surface. Both the anharmonic decay and isotopic scattering rates are high for energetic phonons, but both decrease rapidly with the phonon energy. When the average phonon energy reaches 10 K, the phonon lifetime in a crystalline solid such as silicon is on the order of 100 ms. The isotopic scattering rate for 10 K phonons in silicon is approximately $5\times10^3\ s^{-1}$, resulting in a mean free path on the order of 120 cm. Thus the phonons have a high probability of reaching the surface before thermalizing. It is possible to detect these ballistic phonons, in which case it is the surface area rather than the volume that governs the measured signal. The ballistic phonons can also preserve spatial information about the recoil that would otherwise be lost. This information can be used to define a fiducial volume or to identify the source of the signal. A sensitivity of 1 keV in a full size target has not yet been achieved. The best results to date have been achieved by Colling *et al.*,[3] who reached an energy resolution of 100 eV in a 32-g sapphire crystal using tungsten superconducting transition edge films. It has still to be shown whether the best sensitivity currently available can be maintained when the target mass is increased. Furthermore, even lower thresholds would allow a greater range of target materials. Dark matter detectors with targets of different materials are of interest since the dependence of the event rate and energy deposition on the target nucleus can provide important information about the mass of the dark matter particle. In this paper we discuss the use of a low-temperature amplifier as an alternative approach to increasing the sensitivity.

Ideally, such an amplifier would be sensitive to a single phonon and have good time resolution. In the amplification scheme we propose, the target, a high-quality single crystal of an appropriate material,[2] is covered with a superfluid helium film. The phonons produced by a nuclear recoil, rather than being immediately detected at the target surface, enter the superfluid film and generate excitations in the helium. These excitations have some probability of desorbing helium atoms, which can then be captured on wafers surrounding the target. Each wafer is free of helium on the side facing the target and covered with a superfluid film on the opposite surface. Each helium atom adsorbed onto a bare surface deposits within the wafer a total energy equal to the sum of its binding energy to the solid, typically on the order of 100 K,[4] and its kinetic energy. This energy appears as phonons that may undergo anharmonic decay as they propagate, each producing several lower energy phonons. The phonons reaching the film-covered side of the wafer can create elementary excitations in the helium film, which, in turn, can evaporate more helium atoms. The binding energy of a helium atom to a helium film is only 7 K. Consequently, each helium atom that is adsorbed onto a helium-free surface deposits enough energy that several atoms are potentially evaporated from the

helium film. At each stage, the evaporated helium can be adsorbed onto the helium-free side of the next wafer. After some number of adsorption-evaporation stages, the helium condenses on a final wafer that is bare on both sides. The resulting temperature rise in the final wafer can then be measured and depends on the initial energy deposition. If the efficiency per stage is greater than one, i.e., if more helium is evaporated at each stage than is adsorbed, a proportional amplifier can be constructed. The discovery of cesium as a nonwetting substrate for helium makes the preparation of a wafer with helium on one side a practical possibility.[5–8]

Wurdack, Gunzel, and Kinder[9] proposed a different amplifier based on the evaporation of helium. In their design, the atoms evaporated from a superfluid film are incident on a single plate kept above 50 K. At this temperature, an atom will not stick to the plate. On hitting the hot surface, it is reflected with increased kinetic energy back toward the helium film. The hope was that each atom would then evaporate several additional atoms from the film. If the gain for the evaporation-reflection cycle is greater than one, that is, if each reflected atom evaporates more than one helium atom, the process continues until the entire film evaporates. In experiments carried out by Wurdack *et al.* the initial heat input was generated by a pulsed heater on a silicon substrate coated with a few monolayers of helium. A heated plate was suspended just above the surface by a thin glass fiber. The hot gas resulting from the total evaporation of the film was detected as a large heat pulse to a tunnel junction on the silicon substrate. Wurdack *et al.* found that at input energies of more than 130 pJ (800 MeV), the amplifier worked as described, with a gain per round-trip of 1.8. At lower energy inputs, however, the gain per cycle was less than one so that no heat pulse could be observed.

A number of effects could account for the low efficiency observed for small heat input. The helium atoms incident on the film lose their energy to elementary excitations (phonons, rotons, and ripplons) in the superfluid. The existence of an evaporation threshold, which depends on the number of incident helium atoms, implies that most of the evaporation observed by Wurdack *et al.* is a collective phenomenon associated with these excitations. For a quantum evaporation process, in which a single excitation in the superfluid produces the evaporation of a single helium atom, an excitation must have an energy greater than 7 K. If the spectrum generated by the condensing helium is dominated by low-energy phonons, there may be few excitations satisfying this condition. Even if a significant number of higher energy excitations are produced in the film, the probability that a single phonon or roton will desorb an atom may be low. Above the threshold for amplification, the density of phonons is apparently sufficiently high that a thermal distribution is formed with a significant number of high-energy phonons and rotons in the tail of the Boltzmann distribution.

In our amplification scheme, we try to increase the likelihood of producing higher-energy excitations in the helium by generating the phonons in the solid through the adsorption of the helium atoms onto a film-free surface. Our design has the additional feature that each amplification stage is physically separate. Thus the gain can be controlled and, since the film is never completely evaporated, the dead time should be minimal.

In the next section we describe a series of experiments we have conducted to test this idea and measure the efficiency of the various steps in the proposed amplifier. We then consider the implications of the results to the feasibility of constructing such an amplifier.

II. EXPERIMENTS AND RESULTS

The gain of the proposed amplifier depends on a number of parameters in addition to the ratio of binding energies. A number of distinct steps are required, each potentially involving some energy loss. Among the mechanisms that can decrease the amplification efficiency are the following. (i) Some phonons, generated either by the adsorption of helium or by the nuclear recoil, may have an energy below the 7 K required for quantum evaporation. (ii) Higher-energy phonons that down-convert may produce phonons whose energy falls below 7 K. (iii) The probability of transmission of phonons across the solid-liquid interface is less than unity. (iv) In the liquid, elementary excitations can also down-convert. Again, only excitations reaching the liquid surface with energy greater than 7 K have a nonzero probability of desorbing an atom. (v) Because of restrictions imposed by conservation of parallel momentum at the liquid-vacuum interface, some excitations with sufficient energy cannot cause evaporation. (vi) The probability for quantum evaporation events that are kinematically allowed is less than one. (vii) The sticking probability for an evaporated atom reaching a bare surface is also less than one.

We investigated some of these processes in a series of experiments in which phonons were produced by α particles stopped in a superfluid-coated target. The α particles, emitted by a ^{241}Am source, had a well-defined energy of 5.5 MeV. The width of the energy distribution of the α particles, measured using a surface barrier detector, was 10% due to the americium being embedded within a thin stainless-steel matrix. The helium evaporated by an individual α stopping in the target was condensed on a collection wafer suspended above the target and kept entirely free of helium using a film-burning device.[10] For each α event, the temperature rise in the wafer was measured using a neutron transmutation doped germanium thermistor.[11] Both target and wafer were operated at a base temperature of 25–35 mK in order to maximize the sensitivity of the bolometer and keep the vapor pressure of the helium as low as possible. In these experiments we did not attempt to construct a complete amplifier, but rather to study the processes that would be involved in one.

A. Dependence on target material

In the first experiment we measured the energy deposited in the collection wafers when α particles are stopped in four different targets. We used the following targets: (i) a 1 cm^2, 0.037 cm thick wafer cut from a (111) 78 kΩ cm uncompensated silicon sample supplied by Klitsner;[12] (ii) a similar wafer, cut from the same silicon sample, with a film of 500 Å chromium followed by 2000 Å gold deposited on the upper surface; (iii) a 1×0.7 cm^2, 0.1 cm thick sodium fluoride sample;[13] (iv) and a microscope slide cover glass. The silicon was prepared by cleaning with a 3 min soak in hot trichloroethelene, followed by acetone, methanol, and

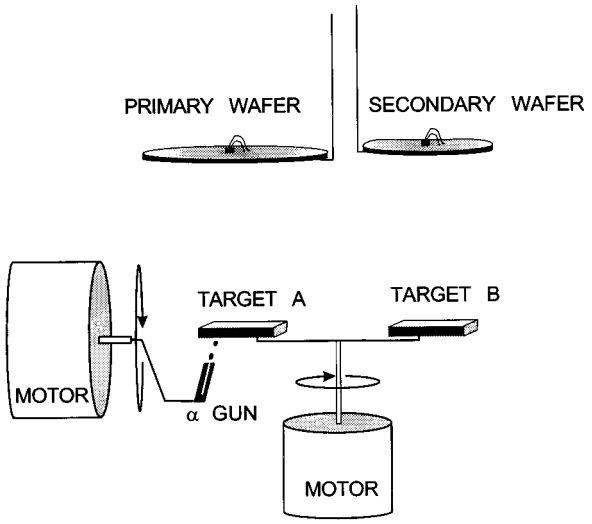

FIG. 1. Arrangement of the cell for the experiment on the evaporation of helium from different substrates. The targets, two of which are shown, are on a carousel that is mounted on a motor. Each target can be rotated into position below the primary wafer. The α source is collimated and mounted on a motor so it can be moved around the target positioned as shown. The evaporation can be measured simultaneously on the two collection wafers.

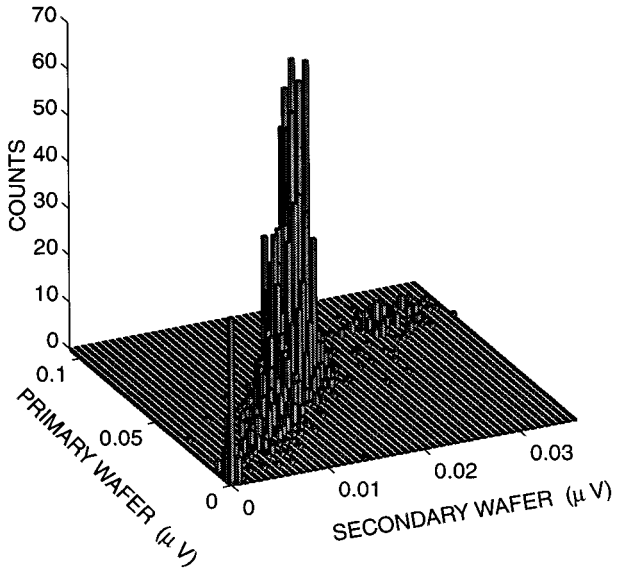

FIG. 2. Histogram plot of the distribution of events as a function of the pulse height in the primary and secondary wafers for evaporation from a silicon target struck by α particles from above at near normal incidence. The pulse heights on the two wafers represent the measured signal in μV on the NTD thermistors at constant bias current. The energy-voltage calibration is different for the two wafers, but is in both cases linear at low energies. On the primary wafer, the signals above the α peak are large enough that the nonlinearity begins to be significant.

deionized water rinses, a hydrofluoric acid dip, and a final deionized water rinse. The glass received the same treatment, except with no acid dip. The NaF target was cleaved just before insertion into the cell and received no further cleaning. The samples were exposed to air for about 2 h while the components were mounted in the experimental cell. The cell was then evacuated and flushed with helium several times. The cell was cooled with an atmosphere of helium introduced at room temperature, a quantity sufficient to form a small pool of bulk helium at the bottom of the cell and coat its contents with a saturated superfluid film.

The cell was arranged as shown in Fig. 1. The samples were mounted on a carousel attached to the shaft of a superconducting stepper motor. Each target could be moved to a position such that it alone could be hit by the α particles. The plane of rotation of the targets was parallel to the helium collection wafers. The α source was collimated to a cone with a half-angle of 5.5° (forming an ''α gun'') and mounted on the shaft of a second, horizontal motor. This motor was positioned so that the gun's axis of rotation was in the plane of the carousel. By moving the source, we were able to direct the α beam at either surface of a target and to vary the angle between the α track and target surface. In order to minimize shadowing of the evaporated helium by the α gun, the primary collection wafer was slightly offset from the target center and the gun was positioned so that the minimum angle of the α's to the surface was about 10° to the normal. As a result, no more than 0.5% of the solid angle subtended by the primary wafer was shadowed by the gun at any orientation. The secondary wafer was not shadowed by the gun at all. The evaporated helium was detected using two collectors: a 20 cm^2 sapphire wafer positioned over the intersection of the α beam with the targets and a 9 cm^2 silicon wafer to the side. The primary (sapphire) wafer subtended a 1.8 sr solid angle above the target. The secondary (silicon) wafer was parallel to the carousel and primary wafer, but offset so that a line from the target to its center made an angle of 50° to the vertical. This wafer subtended a solid angle of 0.34 sr. With certain orientations of the gun and carousel, it was possible for α's to strike the primary helium collection wafer directly. These α's deposited the full 5.5 MeV into the wafer and could be used for energy calibration. As a secondary energy reference, calibrated against the direct α signal, we used the evaporation signals produced by the evaporation of helium from metal film heaters.

The evaporation of helium resulting from an α particle striking a target produces coincident heat pulses in the two wafers. Figure 2 shows the distribution of coincident signals on the primary and secondary wafers for α's hitting the plain silicon target from above at near normal incidence. The spread in the distribution of the coincident signals is approximately equal to the spread in the α-particle energy spectrum. The lower-energy counts are consistent with the rate of the low-energy tail of the α distribution that is due to α particles that have lost a significant fraction of their kinetic energy in the stainless matrix or the collimator. The higher-energy coincident signals are primarily due to two α particles arriving at the silicon within the time resolution of our detector. The majority of events, including both the high- and low-energy signals, falls along a line with a positive slope, indicating that the spatial distribution of the evaporated helium is the same for α particles of different energies and striking different points in the target. Other targets and orientations of the α gun show a similar correlation between the two collection wafer signals.

For each target, the signal was measured with the α's striking the target from above and from below. Measurement

TABLE I. Results of evaporation from different targets. S_{near} is the energy deposited into the primary collection wafer with α's incident on the side facing the wafer. S_{far} is the signal with α's incident on the opposite side. No corrections for solid angle have been made.

Target	S_{near} (MeV)	S_{far} (MeV)	S_{near}/S_{far}
plain Si	8.0 ± 0.3	0.20 ± 0.04	40 ± 8
Si plus metal film	0.7 ± 0.2	0.07 ± 0.04	10 ± 6
NaF	5.0 ± 0.2	0.10 ± 0.03	50 ± 15
glass	8.0 ± 0.3	0.0 ± 0.04	

at low energies was made difficult by the combination of the presence of background pulses produced by γ rays converting in the collection wafers and the intrinsic noise of the system. The background rate increased rapidly with decreasing energy, while at low energies, the noise made the signal on the secondary wafer too small for coincidence measurements to be possible. This made the effective threshold for resolving the evaporation peak on the primary wafer about 70 keV. The energy deposited into the primary wafer for each of the targets is summarized in Table I. The plain silicon target produced the largest signal, with 8.0 MeV deposited in the primary wafer when α's were incident from above the target and 0.20 MeV when α's were incident from below. A metal film on the upper surface of a silicon target drastically reduced this signal. As expected, the glass target, which should be a very poor transmitter of phonons, gave no measurable signal for α's hitting from below. For all targets, the signal produced by α's striking the surface nearest the collection wafer gave a much larger signal than that produced by α's striking from below.

B. Dependence on α track direction

With the same experimental arrangement as shown in Fig. 1, the evaporation from the helium-coated silicon target was measured as a function of the α-particle angle of incidence. In this experiment, the plain silicon target was positioned under the primary collection wafer. The target and collection wafers remained fixed while the α gun was rotated around the target. The signal on the primary wafer was measured as a function of the angle between the normal to the silicon surface and the α track direction. The measured energy into the primary collection wafer as a function of angle for α particles striking the upper surface of the target is shown in Fig. 3. The angle of the gun relative to the target θ is measured from the normal to the target surface. At normal incidence, the energy into the collection wafer is 8 MeV. As the angle from normal incidence increases, the signal monotonically increases. The maximum signal, with the α's incident from above and almost parallel to the target surface, was 12 MeV. For the α's incident from below, the signal is only 210 keV, a factor of 40 down from the maximum signal. Within the accuracy of these measurements, we observed no dependence of the signal size on the gun angle with the α's incident from below the target.

C. Dependence on film thickness

We investigated the dependence of the evaporation signal on the thickness of the helium film. For this experiment, we used a silicon target similar to the one described in Sec. II A with the addition of a neutron transmutation doped thermistor attached to the target. The signal from the thermistor on the target was used as a trigger for signal averaging at the collection wafer. A collimated α source was positioned beneath the target and a helium-free collection wafer was suspended above the target. The apparatus was cooled with no helium in the cell and small increments of helium were added. Although the surface area of the cell and its contents could only be estimated to within a factor of 3, the recovery time of pulsed heaters and the behavior of the film burner verified that even after the first three additions of helium, the resulting film was not superfluid and therefore put an upper bound of approximately 1-ML coverage per addition. After each addition, the evaporation signal was measured. At low coverages no signal was observed. After the fifth addition of helium, a signal appeared and remained constant to within about 30% of the average value with subsequent additions.

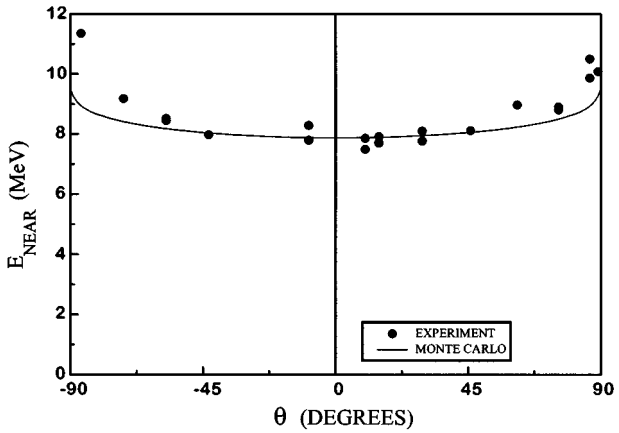

FIG. 3. Energy deposited into the primary wafer by helium evaporated from a silicon target as a function of the incident angle of α particles. The direction of the α track is measured from the normal to the target surface by the angle θ. Points represent data taken with the α source on the same side of the target as the collection wafer. The solid line shows the results of a Monte Carlo calculation (see the text) of the energy into the film with a transmission probability of 0.35 and evaporation efficiency of 0.38.

D. Angular distribution of evaporated helium

In our next experiment, the distribution of the evaporation signal was measured as a function of the angle between the detector and the target. A schematic of this experiment is presented in Fig. 4. A silicon target and an α gun were mounted on the shaft of a motor and positioned between two almost parallel helium collection wafers so that evaporation from both surfaces of the target could be measured in coincidence. In this experiment, the collection wafers were the 9-cm^2 silicon wafer used in Sec. II A and a 1 cm^2 silicon wafer. The target could be rotated in order to vary the angle between the normal to its surface and the collection wafers. The α gun was fixed relative to the target with the beam making an angle of 45° with the normal to the target surface as shown in the figure. This prevented shadowing of the collection wafers by the gun. The signal from the evaporation on the same side as the α beam served as a trigger. By

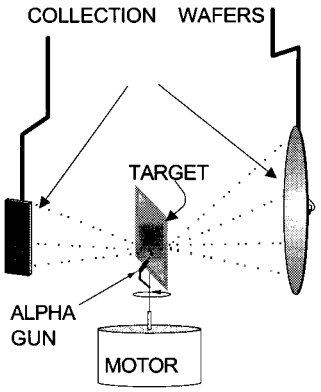

FIG. 4. Schematic of the experimental setup for measuring the spatial distribution of the evaporation from a silicon target. The large signal on the wafer on the same side as the gun is used as a trigger for the other wafer. The gun is mounted at a fixed position relative to the target and is at an angle to prevent shadowing of the signal.

using this trigger and averaging the response on the opposite side, we were able to resolve signals lower than the normal energy threshold. The results of this experiment are shown in Fig. 5, where the energy into the collection wafer per steradian is plotted against the angle between the normal to the target surface and the normal to the collection wafer. On the surface facing the α gun, the 1 cm^2 wafer received a maximum of 4.7 MeV sr^{-1}. The angular dependence is fit well by a cosine function. On the side opposite the gun, the signal was measured using the 9 cm^2 collector. On this side we measure a maximum of 0.1 MeV sr^{-1} and the angular distribution is also well described by a cosine.

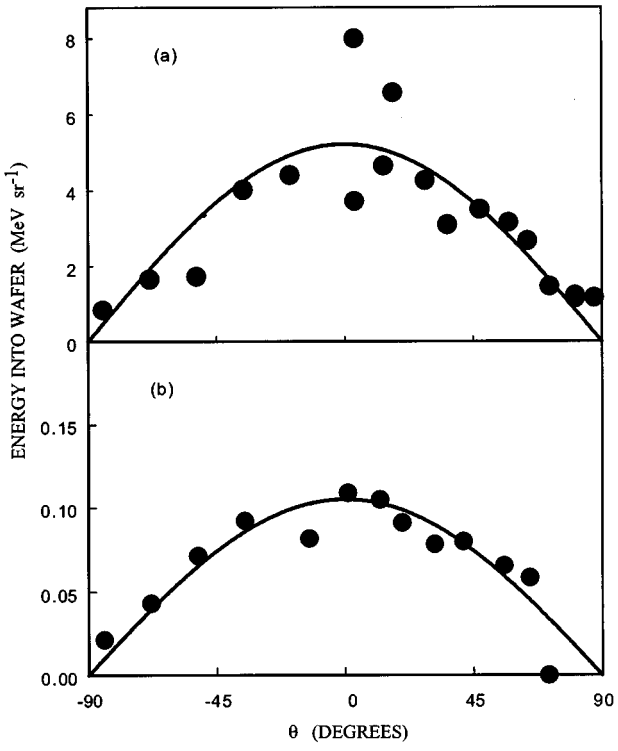

FIG. 5. Energy per unit solid angle deposited into the collection wafer as a function of the angle θ measured from the normal to the silicon target surface. The solid line is the result of a cosine fit to the data points. (a) Evaporation from the same side as the energy deposition. (b) Evaporation from side opposite energy deposition.

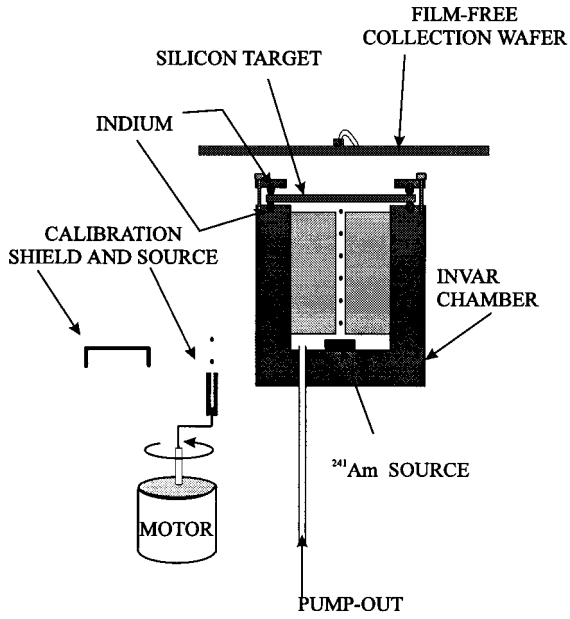

FIG. 6. Schematic of the sealed target experiment. A silicon target is sealed using an indium O ring to an invar chamber. A pump-out tube makes it possible to evacuate the chamber independently of the cell. Helium can also be admitted into the sealed chamber using the pump out. A collimated α source is placed inside the chamber and a film-free collection wafer is placed just above the target. A second ^{241}Am source can be rotated under the collection wafer for calibration or into an enclosed region to isolate it from the experiment.

E. Sealed target experiment

In a final experiment we investigated the desorption due to α's stopped near a film-free surface. For this experiment, a wafer cut from the same (111) silicon used in the previous experiments was sealed by means of an indium O ring to an invar chamber containing a collimated ^{241}Am source (Fig. 6). The chamber had a pump-out tube for both leak testing and introducing helium into the chamber when desired. The α beam was collimated to within 7° of the normal to the silicon surface. The α cone defined a 1 mm radius spot at the center of the silicon. The edge of the indium seal was at a radius of 6 mm. To distribute the forces uniformly and prevent the silicon from breaking, a thin indium washer was placed between the silicon and the thrust plate. Since the silicon was thin and did not make contact with the holder except at the indium, phonons produced by the α particle had to make many reflections at the silicon surfaces before they could escape. Both for the sake of simplicity and for a maximum signal, in this experiment we tried to collect all of the evaporated helium. To this end, a single 20 cm^2 collection wafer was placed as close as possible (1 cm) above the target. A second α source was mounted for calibration on a

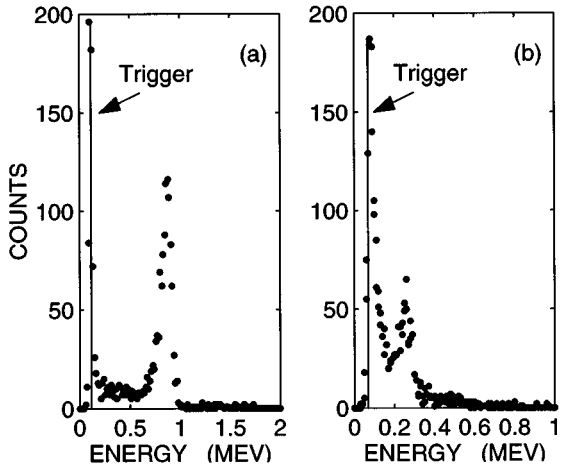

FIG. 7. Pulse height distribution of the evaporation signals in the sealed target experiment. (a) No helium in the sealed chamber. (b) Helium present in the chamber. A pulse is recorded when the change in the voltage across the thermometer exceeds a level indicated by the trigger line on the plots. The lowest energy points at the trigger are due to background.

superconducting stepper motor. The calibration source could be moved under the collection wafer so that α's could hit the wafer directly. When not in use, the source was moved into a shielded area where it could not influence the experiment. An atmosphere of helium was introduced into the experimental cell at room temperature, while the target chamber was kept under vacuum. Upon cooling, the helium condensed to a saturated film on the outer surface of the target, while the surface facing the α source remained free of helium. After measuring the desorption signal with no helium in the test chamber (''vacuum measurement''), enough helium was introduced to form a saturated film on the lower surface of the silicon as well and the evaporation signal was measured again (''helium measurement'').

We measured 880 keV deposited by the evaporated helium adsorbing on the wafer with no helium in the chamber. After helium is introduced to the vacuum chamber so that the target is covered with a helium film on both sides, the energy into the detector wafer drops to 260 keV. Thus we have a factor of 3.4 between the helium and the vacuum measurements. The pulse height distributions for the two measurements are shown in Fig. 7.

F. Summary: Total evaporation from silicon target

We summarize here the evaporation signals measured in the experiments in which a silicon target and saturated helium film were studied. In order to compare the results of the experiments, the measured signal S must be corrected for the solid angle subtended by the collection wafer. In each case, we assume a cosine distribution and estimate S', the integrated evaporation into the two hemispheres defined by the target: the one over the surface facing the α-particle source and the one opposite the source. We have two measurements of the evaporation from the surface near the α-particle impact at near normal incidence with helium on both surfaces. Both the angular distribution measured over the near surface and the α track experiment at normal incidence give 15 MeV as the total energy $S'_{\rm near}$ that would be deposited into a collection wafer covering the full 2π sr solid angle. We also have three measurements from which we can calculate the total adsorption energy into 2π at the far surface $S'_{\rm far}$. In these, the α's were directed at the target at near normal incidence and both surfaces of the target were coated with helium. We find a value of 0.35 MeV for $S'_{\rm far}$ from the angular distribution over the far surface, 0.38 MeV in the experiment on the α track with the source from below, and 0.30 MeV from the sealed target with helium present in the chamber. The sealed target experiment also gives us $S'_{\rm vac}=1.0$ MeV for the integrated evaporation into 2π on the far side when the near side is under vacuum. From the averages of each set of measurements, we can calculate some ratios that will prove useful in analyzing the results. The ratio of the evaporation signal from the side near the α's to the evaporation from the far side with helium on both sides is $S'_{\rm near}/S'_{\rm far}=45$. The ratio of the far side evaporation signal with the near side under vacuum to the far evaporation signal with helium on the near side is $S'_{\rm vac}/S'_{\rm far}=3.4$.

III. DISCUSSION

A. Overview of physical processes

In order to discuss the experimental results, we first present a more detailed description of the principal processes that occur in our experiments between the initial deposition of energy in the silicon target and the final measurement of the heat pulse in the collection wafer. A 5.5 MeV α particle has a range of 25 μm in silicon. It loses its kinetic energy in the silicon primarily by ionization, with the energy loss per unit length increasing as the energy of the particle decreases.[14] For most of its length the α track is essentially straight. The excited electrons produced along the α track lose their kinetic energy by scattering off atoms, thereby generating mostly optical phonons. These phonons decay into lower-energy acoustic phonons, which then continue to decay further at a rate that depends on the phonon energy as $E_{\rm ph}^5$.[15] At the same time, the phonons scatter elastically at a rate proportional to $E_{\rm ph}^4$ from isotopic impurities.[16] The effect of these two processes in which the diffusivity is increasing in time while the mean energy decreases is known as quasidiffusion.[15,17,18] When a phonon reaches the surface of the silicon and there is liquid helium on the other side of the interface, transmission of energy via the excitation of phonons and rotons in the liquid occurs with a probability that depends on the surface conditions.[19,20] If no helium is present, the phonons are expected to reflect specularly. At a real surface that has an oxide layer, adsorbed material, or damage, the reflection may have a diffuse component. The phonons may also down-convert in the oxide layer before returning to the silicon.

Of the energy that enters the helium film, only a fraction leads to evaporation. The energy appears in the helium as rotons and phonons. The evaporation from the surface of bulk helium at low temperatures has been shown by Wyatt[21–23] to be dominated by quantum evaporation processes. The term quantum evaporation is used by Wyatt to

indicate that in the evaporation event, a single excitation gives up all of its energy to a single helium atom. When a roton or phonon arrives at the free surface, it will often reflect instead of desorbing an atom. Excitations may also down-convert, resulting in phonons with energy too low to cause evaporation. At the solid interface, the excitations may return into the silicon. If the temperature rise in the helium is sufficiently high, interactions among the excitations will maintain a thermal distribution of rotons. The lower-energy phonons produced by the decay of rotons will recombine to replenish the roton bath and a larger fraction of the energy entering the helium will produce evaporation.

Because of geometric constraints in assembling the experiments, not all of the evaporated helium atoms reach the collection wafers. The evaporated atoms that do arrive at the bare surface of a collection wafer have a certain probability of sticking to it and depositing their kinetic and binding energies. Both the sticking probability and the binding energy to the solid depend on the wafer material. The sticking probability will also depend on the energy of the incident helium atoms.

In the discussion that follows, we will denote the total energy deposited into a helium film on the near surface (on which the α particle is incident) as Q_{near} and the energy in the far film when both surfaces are coated with helium as Q_{far}. When the near surface is under vacuum the energy in the far film will be Q_{vac}. Similarly, the total energy that would have been measured by a bare wafer covering the full 2π region over the near surface will be S'_{near}. The total energy that would be measured at the far wafer when helium is present on both surfaces will be S'_{far} and the energy measured at the far wafer when the near film is under vacuum will be S'_{vac}.

B. Phonons in silicon

In most of our experiments, the target is a thin silicon wafer with a helium film covering both of its principal surfaces. The fraction of the α particle's energy that is deposited in the helium at each surface depends on the direction of the α track, the rates governing the quasidiffusion of the phonons, and the probability of transmission of phonons across the silicon-helium interfaces. The α particle generates high-energy phonons close to the surface at which it enters. The mean free path of these phonons is initially very short. As the phonons decay, the mean free path increases and eventually becomes comparable to the thickness of the target. Most of the phonons that reach the far side of the wafer will have had to reflect at the near surface several times. Each time they reach a helium covered surface, they have some probability of losing their energy to the liquid. We have carried out a Monte Carlo calculation in order to estimate the fraction of the energy that is deposited in the helium at the near surface. We consider the propagation of phonons produced by a 5.5 MeV α particle stopped in a 370 μm thick silicon target. The energy arriving at the near film is calculated for several assumed values of the probability for the transmission of phonons into the helium and for a range of α track directions.

We begin with the energy distribution expected for ionization along a straight 25 μm track lying in the same direction as the incident α momentum. The energy loss of a heavy particle of charge Ze, mass m, and velocity v in a medium containing N electrons per cm^3 has been calculated by Bethe and is given by[14]

$$-\frac{dE}{dx}=\frac{4\pi Z^2e^4}{mv^2}N\left[\ln\frac{2mv^2}{\left(1-\frac{v^2}{c^2}\right)I}-\frac{v^2}{c^2}\right]. \tag{1}$$

Here I is a characteristic energy for the stopping material and is approximately 170 eV for silicon. In calculating the quasidiffusion of the phonons, we follow the derivation given by Maris.[15] We assume that all of the energy appears as phonons of sufficiently high energy that their lifetime is short; we choose an initial energy of 800 K for all the phonons, but the dependence of the results on the starting energy is weak as long as the mean free path at the initial energy is much less than the depth to which the α particle penetrated. The isotopic scattering rate in silicon is taken as[15]

$$\tau_I^{-1}=0.46E_{\text{ph}}^4\ \text{s}^{-1}\ \text{K}^{-4} \tag{2}$$

and the anharmonic decay rate as

$$\tau_A^{-1}=1.6\times10^{-4}E_{\text{ph}}^5\ \text{s}^{-1}\ \text{K}^{-5}, \tag{3}$$

where the phonon energy E_{ph} is measured in kelvin and the decay rate is averaged over the longitudinal and transverse phonon modes. When a phonon decays, the two resulting phonons are taken to be collinear, but not necessarily of equal energies. The probability that a phonon of energy E_{ph} decays into one phonon of energy xE_{ph} and the other of energy $(1-x)E_{\text{ph}}$ is taken to be proportional to

$$x^2(1-x)^2. \tag{4}$$

For the propagation of the phonons between scatterings and decays, we neglect the anisotropy in the sound velocity and assume that all the phonons travel at the Debye velocity. At the surface, there is a probability P_{trans} that the phonon energy is transmitted into the helium. Since the transmission of phonons from a solid into liquid helium depends on the surface conditions, P_{trans} is taken as an adjustable parameter in the program. The transmission across the interface is assumed to be independent of the phonon energy and angle of incidence. Phonons that are not transmitted are assumed to reflect diffusely. We do not consider any other loss mechanisms at the surface or within the silicon crystal.

Figure 8 shows the calculated energy that enters the near film as a function of the direction of the α track for several values of P_{trans}. The track direction is measured from the normal to the target surface by the angle θ. As the probability of transmission increases, the fraction of the energy that enters the helium at the near surface also increases. As θ increases, the energy is deposited closer to the target surface and a greater fraction enters the near film.

By comparing the calculated energy deposition at normal incidence to the results of the sealed target experiment, we can estimate the transmission probability P_{trans}. We measured a ratio of 3.4 between the evaporation signal with the sealed chamber evacuated and the signal with helium present in the chamber. In both cases, the phonons must travel approximately the same distance to arrive at the surface at

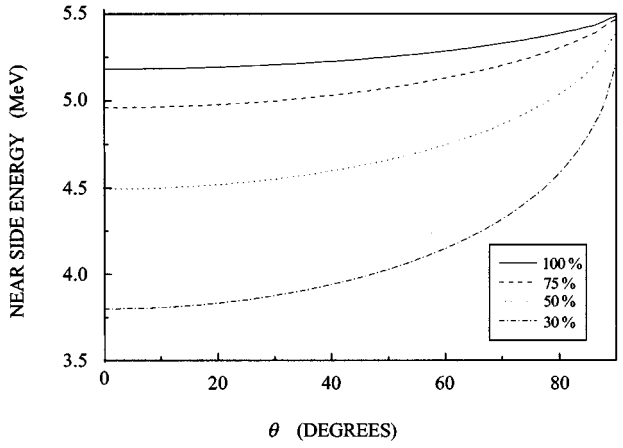

FIG. 8. Energy entering the near helium film as a function of the angle of incidence of the α particle, θ, as measured from the normal to the target surface. Curves are the results of a Monte Carlo calculation with different transmission probabilities, as indicated.

which the evaporation is measured. Any energy losses within the bulk silicon should therefore attenuate both signals equally. As long as the losses at the vacuum-solid interface are not significant, the ratio of the energies entering the film in the vacuum and helium measurements $Q_{\rm vac}/Q_{\rm far}$ should then be equal to the ratio of the full kinetic energy of the α particle to the calculated energy entering the far film with a film on the near surface $E_\alpha/Q_{\rm far}$. We will see Secs. III C and III D that in the case of the far film, the ratio between the energy entering the film and the energy deposited in the collection wafer should not depend on the conditions present at the near surface. If we assume that $S'_{\rm vac}/S'_{\rm far}$ is equal to $Q_{\rm vac}/Q_{\rm far}$, the experimentally measured ratio best agrees with the Monte Carlo calculation at $\theta=0$ when the transmission probability $P_{\rm trans}$ is taken to be 0.35.

The quasidiffusion model has recently been experimentally verified by Shields, Msall, Carroll, and Wolfe,[24,25] who performed an experiment in which phonons produced near a silicon surface undergo quasidiffusion. Shields *et al.* used 10 ns Ar^+ laser pulses to generate phonons in silicon and measured the phonon signal arriving at a bolometer on the surface opposite from the excitation surface. The signal was measured first with the excitation surface under vacuum and then with it in contact with bulk helium. The surface at which the signal was measured was always in contact with helium. When high-energy phonons were produced, Shields *et al.* found good agreement with a Monte Carlo calculation similar to the one presented above. The experiments support the quasidiffusion model as well as provide a measurement of $P_{\rm trans}=0.5$ for the silicon-helium interface of their sample. This value is higher than our estimate of 0.35 for the transmission probability, but both values are well within the expected range for an untreated silicon surface.[19]

C. Evaporation efficiencies

We define the evaporation efficiency as

$$e\equiv\frac{N\epsilon_{\rm liq}}{Q}, \tag{5}$$

where N is the number of helium atoms that are desorbed, $\epsilon_{\rm liq}$ is the binding energy of a helium atom to the helium film, and Q is the total energy deposited in the helium film. The energy that would be deposited in a collection wafer covering the full 2π hemisphere over the target surface is

$$S=N(\epsilon_{\rm solid}+\epsilon_{\rm kin})\alpha. \tag{6}$$

Here $\epsilon_{\rm solid}$ is the binding energy of the helium atoms to the bare collection wafer, $\epsilon_{\rm kin}$ is the average kinetic energy per atom of the evaporated helium, and α is the probability that a helium atom arriving at the collection wafer will stick to it. From Eqs. (5) and (6), we can express the efficiency as

$$e=\frac{S}{Q}\frac{\epsilon_{\rm liq}}{(\epsilon_{\rm solid}+\epsilon_{\rm kin})\alpha}. \tag{7}$$

We have reported elsewhere[26] measurements of the factor

$$f\equiv\frac{\epsilon_{\rm liq}}{(\epsilon_{\rm solid}+\epsilon_{\rm kin})\alpha} \tag{8}$$

for evaporation by rotons near the dispersion minimum in bulk helium. For the silicon and sapphire wafers used in the experiments discussed in this paper, we found the value $f\approx0.10$. We will assume that the same value of f applies in the present experiments. The principal concern regarding this assumption involves the probability of helium sticking to the collection wafers; the sticking probability could be different in the two experiments due to differences in surface conditions and in the energy spectrum of evaporated atoms.

We calculate the efficiency $e_{\rm vac}$ at the far surface from the results of the sealed target experiment with no helium present, the above value for f, and Eq. (7). The experimental value for the energy $S'_{\rm vac}$ deposited in the collection wafers is 1.0 MeV, as discussed in Sec. II E. The energy transmitted into the film when the sealed chamber is evacuated is the full kinetic energy of the α particle, 5.5 MeV. Thus we find that the efficiency of evaporation from the far surface is $e_{\rm vac}=1.0\times0.10/5.5=0.018$. As we will discuss in Sec. III D, it is reasonable to assume that the evaporation efficiency on the far side does not depend on the conditions if the near side. That is, the efficiency with helium present on the near surface $e_{\rm far}$ is the same as $e_{\rm vac}$.

We get a very different result for the efficiency at the near surface $e_{\rm near}$. In Sec. III D we will argue that the efficiency of evaporation at the far surface is the same regardless of the presence of helium on the near surface. From the sealed target experiment we can therefore find the energy transmitted to the helium at the far surface of the target ($Q_{\rm far}$) when helium is present on both sides:

$$Q_{\rm far}=\frac{S'_{\rm far}}{S'_{\rm vac}}E_{\rm alpha}, \tag{9}$$

where E_α is the kinetic energy of the α particle. $S'_{\rm far}$ is the energy deposited into the collection wafers, as summarized in Sec. II F. Equation (9) gives $Q_{\rm far}=1.6$ MeV. The α energy that is not transmitted to the far film appears in the near film, so that

$$Q_{\rm near}=E_\alpha-Q_{\rm far}. \tag{10}$$

The energy in the near film at normal incidence is therefore 3.9 MeV. The measured signal on the near side S'_{near} was measured in both the angular distribution and the α direction experiments. These results are given in Sec. II F. Using these values for S and the calculated energy input of 3.9 MeV for Q in Eq. (7), we find that the evaporation efficiency at the near surface e_{near} is 0.38.

The ratio of evaporation efficiencies at the near and far surfaces $0.38/0.018 \approx 20$ is too large to be explained by any uncertainty in the parameters in the Monte Carlo model. According to this model, the maximum energy deposition to the near film occurs for perfect transmission of the phonons across the silicon-helium interface. If this occurred, the Monte Carlo simulation predicts 4.7 MeV entering the near film and 0.80 MeV entering the far film. Combining these values for Q with the measured values for S, we would then find a near efficiency of 0.32 and a far efficiency of 0.044. Thus the evaporation from the near surface is still more than an order of magnitude more efficient than the evaporation from the far surface. For the source of this discrepancy, we consider in greater detail the distribution of the energy that is deposited in the helium at the two surfaces and the resulting evaporation rates.

D. Superfluid film

We believe that the difference in efficiencies is related to differences in the energy density in the helium films covering the near and far surfaces. In this section we present the evidence in favor of this view.

Let us first consider the processes that occur when a *small* flux of phonons is incident from the silicon onto a helium film. Some of these excitations will enter the film and appear there as rotons and phonons. The energy spectrum of these excitations in the helium film is not known. It may be significantly affected by the condition of the silicon surface. The oxide layer, for example, may absorb the incident phonons and reemit them into the helium film with a substantially lower energy. One expects that because the density of states for rotons is much larger than for phonons, most of the excitations in the film will be rotons.

Once in the film the excitations will propagate across and impinge on the free surface. For each excitation of momentum $\mathbf{p}$ there will be a probability $P(\mathbf{p})$ of evaporation. The functional form of $P(\mathbf{p})$ is not known in quantitative detail, but some characteristic features have been established. Excitations of energy below 7.2 K (from the phonon part of the spectrum) do not have enough energy to cause evaporation and so P must be zero. For excitations above the energy threshold, Wyatt[21] has shown that the energy and the component of the momentum parallel to the surface are conserved in the evaporation process. Because of these conservation laws, only rotons that are incident on the superfluid surface within a certain angle of the normal can lead to evaporation. For rotons with momenta close to the roton minimum this angle is approximately 20°. If the roton velocities are uniformly distributed over all directions, the probability that an incident roton will lie within this allowed range of directions is 0.060. We have reported[27] a lower bound of ~ 0.35 for the probability of evaporation by rotons at approximately normal incidence to the surface of bulk helium and with energy near the roton minimum. For want of a better estimate, we assume that this same probability applies for *all* rotons within the angular range allowed by the conservation laws and that the probability is zero for larger angles. The evaporation probability per single encounter with the surface P_{single} is therefore $0.35 \times 0.060 \sim 0.021$.

Those rotons that are reflected from the free surface of the film will return to the helium-silicon interface. At this interface a roton may be reflected as a roton, reflected as a phonon, reflected as multiple excitations, or transmitted into the silicon. If transmission into the silicon occurs, the energy in the roton will not contribute to the evaporation. If the energy is reflected back into the helium film as multiple excitations, the chance of evaporation occurring is reduced because the excitations may have too low an energy to cause evaporation. The relative probabilities of the different possible processes at the helium-silicon interface are not understood. In an experiment with bulk helium[28,29] we have compared the evaporation by a pulse of rotons directed at the free surface of the liquid with the evaporation measured after the rotons were reflected at a silicon surface. The ratio of the evaporation signals was found to be 0.3. If we accept this value as a reasonable approximation to the effective roton reflection coefficient r in the present experiment, we can calculate the evaporation probability P_{mult} allowing for multiple attempts to be

$$P_{\text{mult}} = \frac{P_{\text{single}}}{1 - r(1 - P_{\text{single}})} = 0.03. \tag{11}$$

This result is in reasonable agreement with the evaporation efficiency that we have measured at the far surface (0.018).

This calculation assumes that there are no interactions *between* the excitations while they are in the film. Thus, for example, we have considered that rotons may decay into lower-energy excitations (phonons) when they return to the helium-silicon interface, but the regeneration of rotons by coalescence of the lower-energy excitations has been neglected. If these coalescence processes occur at a sufficient rate they will lead to a distribution of excitations characterized by some effective temperature T. If this temperature is sufficiently high the evaporation efficiency will increase. We believe that the onset of this ''thermal'' evaporation is the reason that we measure a much larger evaporation efficiency at the film on the near surface.

In order for there to be a high efficiency of evaporation by a thermalized distribution of excitations it is necessary that the rate of escape of energy $\dot{Q}_{\text{evap}}(T)$ from the film as a result of evaporation be greater than the rate $\dot{Q}_{\text{Si}}(T)$ due to the energy loss back into the silicon substrate. To estimate $\dot{Q}_{\text{evap}}$ we note that when helium liquid is in contact with saturated vapor at the same temperature T the rates at which atoms condense from the gas and evaporate from the liquid must be equal. The flux of atoms from the gas side is

$$\frac{1}{4} A n_{\text{gas}}(T) v_{\text{gas}}(T), \tag{12}$$

where A is the area considered, n_{gas} is the density in the gas, and $v_{\text{gas}} = (8kT/\pi m)^{1/2}$ is the average atomic velocity in the gas. Since the probability of an incident gas atom condensing

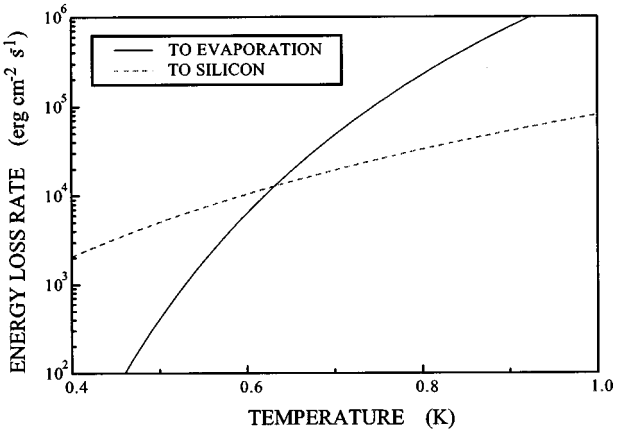

FIG. 9. Calculated energy-loss rate from a helium film by evaporation and by phonon radiation into the substrate as a function of temperature.

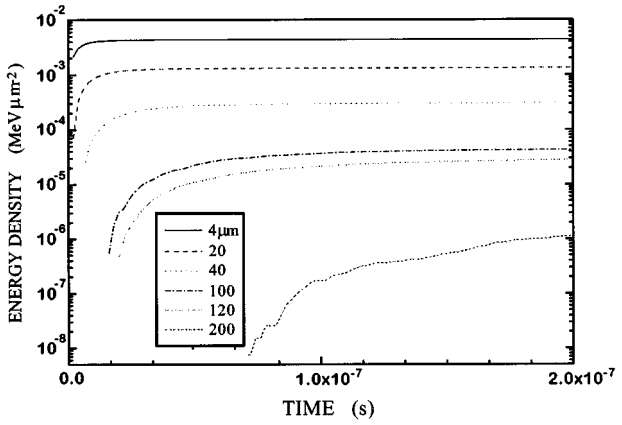

FIG. 10. Energy deposited per unit area of the film for various distances from the α track as estimated from the Monte Carlo simulation. The track is assumed to be perpendicular to the silicon surface. The quantity plotted is the energy per unit area integrated over time up to the time indicated.

into the liquid is close to unity,[30] we can assume that essentially all of these atoms enter the liquid. It follows that the rate at which atoms evaporate from the liquid must be given by this same expression. If we now consider a situation in which the liquid is at temperature T and there is no vapor above it, the rate of energy loss from the liquid will be

$$\dot{Q}_{\rm evap}=\frac{1}{4}An_{\rm gas}(T)v_{\rm gas}(T)L, \tag{13}$$

where L is the binding energy of helium, i.e., 7 K. An analogous calculation can be made to estimate the rate at which heat flows from the film into the silicon. The result is

$$\dot{Q}_{\rm Si}=\frac{1}{4}AE_{\rm Si}(T)v_{\rm Debye}P_{\rm trans}. \tag{14}$$

In this expression $P_{\rm trans}$ is the average phonon transmission probability for phonons going from silicon into the film, $E_{\rm Si}$ is the energy density in silicon at temperature T, and $v_{\rm Debye}$ is the Debye average sound velocity. For $P_{\rm trans}$ we will use the same value (0.35) estimated in Sec. III B. In Fig. 9 we show $\dot{Q}_{\rm evap}$ and $\dot{Q}_{\rm Si}$ as a function of temperature. It can be seen that above 0.64 K the heat loss by evaporation is larger than the loss due to phonon radiation.

It follows from this result that for thermal evaporation to give a high efficiency the film must be heated above 0.64 K. It is straightforward to estimate the energy input required to do this. We assume that the film thickness is 300 Å and obtain the result that the energy per unit area needed to reach 0.64 K is 2×10^{-5} MeV μm^{-2}. We can compare this value with the energy deposited per unit area of the film as given by the Monte Carlo calculation. Figure 10 shows the calculated energy deposit into the helium on the near surface per unit area for different distances from the point where a track at normal incidence intersects the silicon surface. Even at distances as far as 120 μm from the track the temperature rise of the film exceeds the crossover temperature 0.64 K. At the far surface, the maximum energy density predicted by the Monte Carlo calculation is less than 2×10^{-6} MeV μm^{-2}, even when the near side is under vacuum and the full 5.5 MeV deposited in the silicon enters the far film. Thus, at no point does the temperature of any part of the far film exceed the crossover temperature.

It is important to note that the calculation just given implicitly assumes that the energy arrives at the film on a time scale short compared to the time for evaporation to occur. We can define this time as

$$\tau_{\rm evap}=Q(T)/\dot{Q}_{\rm evap}(T), \tag{15}$$

where Q is the thermal energy in the film needed to raise its temperature to T. This time is 200 ns at 0.64 K and is thus considerably longer than the time it takes for most of the energy from the α particle to reach the film (see Fig. 10). At higher temperatures the time decreases and becomes comparable to the time over which energy is deposited. Thus, for those regions of the film that receive large amounts of energy per unit area some of the energy will be lost by evaporation before all of the energy has arrived. The helium temperature will not reach the maximum value calculated from the energy density, but will still be high enough for evaporative heat loss to dominate over substrate phonon reemission.

IV. CONCLUSIONS

In order to construct a useful amplifier based on the evaporation of helium, the gain — the energy received in the collector divided by the initial energy deposited by the particle S/Q — must be greater than unity. This condition is clearly not met in the present experiments for the geometry of interest. When helium is evaporated from the far surface with no helium film on the near surface, $S/Q=1.0/5.5=0.18$. (The fact that S/Q is greater than one when helium is evaporated from a local hot spot produced by an α particle at the near surface is of no consequence to the design of an amplifier, where the energy density can be expected to be low.)

Several factors may contribute to the low value of the gain. These include (i) down-conversion of phonons in the solid to energies below the threshold for quantum evaporation, (ii) poor transmission of phonons across the solid-liquid

interface, (iii) low probability of a helium atom being evaporated by a roton in a single encounter with the surface of the liquid film, and (iv) loss of rotons upon their interaction with the solid interface. Our calculation of the phonon quasidiffusion and transmission into the helium suggests that (i) and (ii) are not significant problems. We believe that the combination of (iii) and (iv) is principally responsible for the low gain.

With the discovery of substrates to which helium is only weakly bound[5–8] it may be possible to avoid the losses associated with the saturated superfluid film. Atoms can be desorbed directly from a weakly bound monolayer on the surface of the solid. Helium is expected to be bound to cesium with an energy of only a few degrees kelvin.[31] However, the mobility of weakly bound helium atoms is likely to be high and the binding of helium to itself is stronger than the binding to cesium. It may not be possible to maintain a monolayer of ^{4}He on a thick cesium substrate at low temperatures. On the other hand, liquid ^{3}He does wet cesium, the binding energy of an atom to the liquid being only 2.5 K. With ^{3}He a stable monolayer should be obtainable at low temperatures, if not on a thick cesium substrate then on a thin cesium substrate. The binding energy to the surface can be tuned to a desired value as a consequence of its dependence on the cesium thickness.[32]

The use of a weakly bound monolayer of helium may make it possible to construct an amplifier with useful gain. In the present experiments an overall gain of 0.18 was obtained when the probability of desorbing a helium atom from the film by a roton was 0.025 [Eq. (11)]. To achieve a gain of greater than 1 the probability of a phonon desorbing a helium atom from the monolayer would need to be larger, roughly, than 0.14. This estimate does not take into account the possible difference in number of phonons with energies sufficient to desorb atoms from a monolayer and the number of excitations in the film capable of evaporating atoms. We are not aware of any theoretical calculations or experimental measurements that provide any direct information about the probability of a phonon desorbing an adsorbed helium atom. However, observations by Irwin[33] indicate that phonons in silicon couple very efficiently to an adsorbed monolayer of helium. Irwin studied the ballistic phonon signal arriving at a thin-film bolometer on the surface of a silicon crystal. The signal, resulting principally from phonons that are reflected from the silicon surfaces prior to reaching the bolometer, is strongly attenuated if a monolayer of helium is adsorbed on the silicon. In Irwin's experiment the phonon energies are unlikely to be sufficiently large to produce desorption of helium from the silicon, but rather create excitations of the atoms bound to the surface. Because of the strong interaction between phonons and adsorbed atoms the probability may be high for desorbing ^{3}He atoms from a cesiated surface with much lower binding energies. Thus the development of a useful amplifier for particle detection remains a possibility.

ACKNOWLEDGMENTS

This work has been supported by the U.S. Department of Energy under Grant No. DE-FG02-88ER40452 and by the National Science Foundation through the Center for Particle Astrophysics at the University of California, Berkeley. T.M. acknowledges support from the U. S. Department of Education.

*Present address: Universität Heidelberg, Heidelberg, Germany.
† Present address: Universität Karlsruhe, Karlsruhe, Germany.

[1] See articles in *Proceedings of the Fifth International Workshop on Low Temperature Detectors* [J. Low Temp. Phys. **93** (3/4) (1993)].
[2] P. F. Smith and J. D. Lewin, Phys. Rep. **187**, 203 (1990).
[3] P. Colling *et al.* (unpublished).
[4] G. Vidali, G. Ihm, H.-Y. Kim, and M. W. Cole, Surf. Sci. Rep. **12**, 133 (1991).
[5] E. Cheng, M. W. Cole, W. F. Saam, and J. Treiner, Phys. Rev. Lett. **67**, 1007 (1991).
[6] P. J. Nacher and J. Dupont-Roc, Phys. Rev. Lett. **67**, 2966 (1991).
[7] K. S. Ketola, S. Wang, and R. B. Hallock, Phys. Rev. Lett. **68**, 201 (1992).
[8] P. Stefanyi, J. Klier, and A. F. G. Wyatt, Phys. Rev. Lett. **73**, 692 (1994).
[9] S. Wurdack, P. Gunzel, and H. Kinder, in *Phonons 89*, edited by S. Hunklinger, W. Ludwig, and G. Weiss (World Scientific, Singapore, 1989), pp. 1394–1396.
[10] R. Torii *et al.*, Rev. Sci. Instrum. **63**, 230 (1992).
[11] The NTD chip was provided by E. E. Haller of Lawrence Berkeley Laboratory, Berkeley, California.
[12] T. Klitsner, Sandia National Lab, Albuquerque, New Mexico.
[13] Cleaved from a sample supplied by Optovac, North Brookfield, Massachusetts. The NaF was 99.99% pure and had not been irradiated.
[14] E. Segrè, *Nuclei and Particles*, 2nd ed. (Benjamin/Cummings, Reading, MA, 1977).
[15] H. J. Maris, Phys. Rev. B **41**, 9736 (1990).
[16] S. Tamura, Phys. Rev. B **27**, 858 (1983).
[17] V. Kazakovtsev and Y. B. Levinson, Phys. Status Solidi B **96**, 117 (1979).
[18] S. Tamura, J. Low Temp. Phys. **93**, 433 (1993).
[19] J. R. Olson and R. O. Pohl, J. Low Temp. Phys. **94**, 539 (1994).
[20] L. Koester *et al.*, Z. Phys. B **80**, 275 (1990).
[21] A. F. G. Wyatt, Physica B+C **126B**, 392 (1984).
[22] G. M. Wyborn and A. F. G. Wyatt, Phys. Rev. Lett. **65**, 345 (1990).
[23] A. F. G. Wyatt, J. Low Temp. Phys. **87**, 453 (1992).
[24] J. A. Shields, M. E. Msall, M. S. Carroll, and J. P. Wolfe, Phys. Rev. B **47**, 12 510 (1993).
[25] S. E. Esipov, Phys. Rev. B **49**, 716 (1994).
[26] F. S. Porter, Ph.D. thesis, Brown University, 1994.
[27] C. Enss *et al.*, *Proceedings of the 20th International Conference on Low Temperature Physics* [Physica B **194-196**, 515 (1993)].
[28] S. R. Bandler, Ph.D. thesis, Brown University, 1994.
[29] S. R. Bandler *et al.*, Phys. Rev. Lett. **74**, 3169 (1995).
[30] D. O. Edwards *et al.*, Phys. Rev. Lett. **34**, 1153 (1975).
[31] M. Cole (private communication).
[32] P. Taborek and J. E. Rutledge, Phys. Rev. Lett. **71**, 263 (1993).
[33] K. Irwin, Ph.D. thesis, Stanford University, 1995.